

Self-sensing Sustainable Cementitious Mixtures Incorporating Carbon Fibres

Thamer Almotlaq^{1,2}, Mohamed Saafi¹

¹School of Engineering, Lancaster University, Lancaster, LA1 4YR, UK.

²Civil Engineering department, College of Engineering, Jouf University, Sakaka 72388, Saudi Arabia.

Abstract. This paper focuses on sustainable cementitious composites in terms of their conductivity, hydration and self-sensing properties, which are key features for smart city infrastructures. Smart cities have massive infrastructures that are interconnected, transmitting data and information for health-monitoring and performance optimization. In this regard, having them made of sustainable building materials (concrete) that are also sufficiently conductive, will be a suitable solution for structures' performance. The studied sustainable cementitious mixtures are made by sea components (sea water and sea sand), which are abundant resources. The primary goal of this study is to improve the mixes' electrical conductivity and sensitivity. To achieve this goal, milled carbon fibres (MCFs) and chopped carbon fibres (CCFs) in 6 different proportions were added to the cementitious mixes. The experimental study is divided into impedance spectroscopy to study the conductivity and hydration development, and self-sensing properties, conducted on various mix designs. The results show that incorporating sea components improve the electrical conductivity of the mixes by 40-50%. Further improvements were achieved by adding MCF as it shows a remarkable reduction by 60% compared to the plain ss-sw (sea sand and sea water) samples. Adding CCF improved the conductivity even further and resulted in sample's resistivity as low as 53 Ω cm after 1 year of curing time.

1. Introduction

Concrete is a highly significant construction material because of its durability, versatility, and reliability. Presently, sustainable construction has an increasing demand globally, mainly because of growing environmental concerns such as global warming, climate change, pollution, etc. Thus, the emphasis is currently on moving towards making concrete and construction materials which are comparatively less damaging to the environment [1, 2]. The mixture of concrete uses natural resources which are gradually depleting. Globally, gravels and sand that are used in the mixtures are extracted from the crust of the earth through legal and illegal mining, therefore, damaging the ecosystem [3, 4]. Freshwater is another natural resource used in concrete, and is depleting rapidly because of its extensive use. The excessive consumption of fresh water in making concrete results in the reduction of drinkable water to around 40% of the global population [5, 6].

Sea sand and seawater can be the solution to such problems [7, 8]. According to [9], it was observed that seawater comprises 96.5% of earth's total water that can be used instead of fresh water for making concrete. In addition, sea sand is similarly available in large quantities and can be used as a sustainable resource for concrete production.

Moreover, smart cities are turning into a reality, which involves massive infrastructures that are interrelated, transmitting information and data for performance optimization. The features of such cities are to have monitoring and surveillance equipment on buildings, bridges, and roads. From this point of view, having conductive concrete structures will possibly be a

sustainable and suitable and possibly a more accurate solution for structures' health monitoring instruments for transmitting signals and data. [10, 11].

This paper focuses on providing an answer to have a sustainable concrete mixture, which can be employed in smart city infrastructures and in particular, health monitoring facilities. In order to make the mixes sustainable, sea components, are employed in the mixes, and the primary property to be improved is the mixes' conductivity and sensitivity. Improving the conductivity of the cement mortar mixes is done through incorporating certain admixtures of carbon fibre in milled and chopped forms. Both materials are relatively cheap, commercially available and are expected to improve the conductivity and sensitivity of the mixes. In the current phase of this research, several cement composite mixes are made using the mentioned admixtures and their conductivity properties are experimentally studied.

2. Experimental program

2.1. Materials and mix designs

Ordinary Portland cement (OPC) of 32.5 R from Blue Circle, was used throughout the experimental study as the binder. Normal sand was used only in the reference samples, and in the rest of the samples, sea sand was employed. Based on the literature [11, 12], the mortar's aggregate to cement (a/c) and water to cement (w/c) ratios were 1.5 and 0.5, respectively. Moreover, two types of carbon fibre were used, in 3 different concentrations. Tables 1 and 2 show the OPC's chemical components and material properties of the two types of carbon fibres, respectively. Both carbon fibres were added at 0, 1, 2 and 2.5% by weight of cement. Based on preliminary experimental observations, these

percentages show better results in terms of improving electrical properties [11, 13-15]. Figure 1 shows a sample of the carbon fibres' scanning electron microscope (SEM) and energy dispersive X-Ray (EDX).

Table 1: Chemical components of OPC.

Chemical Elements	By mass (%)
SiO ₂	20.38
Al ₂ O ₃	5.4
Fe ₂ O ₃	2.82
CaO	63.04
MgO	1.74
Loss of ignition	1.66

Table 2: Carbon fibres properties

Commercial Name	Cabriso Powder	Easy Composite
Average Diameter	7 µm	-
Average Length	80/100 µm	12 mm
Density	1800 kg/m ³	1.8 g/cm ³
Tensile Modulus	200 GPa	4-5 GPa
Gross Weight	0.065 kg	0.435 kg
Price (£/kg)	32.00	39.00

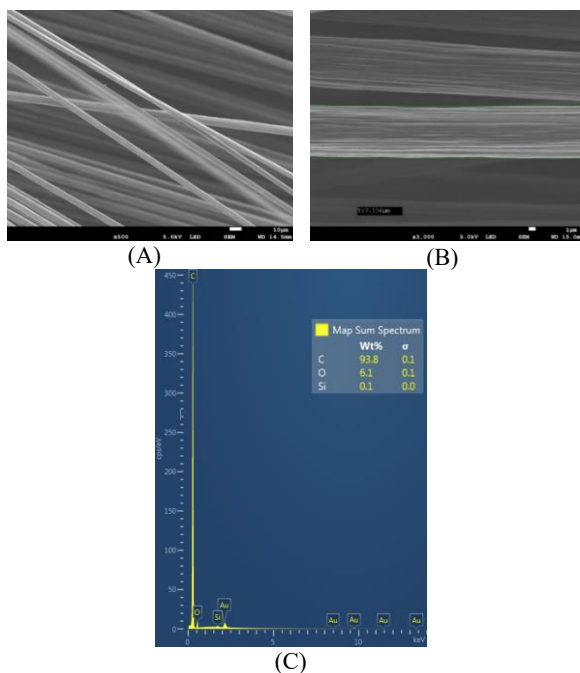


Fig. 1: (A) and (B) are SEM, (C) is EDX of carbon fibres.

In some samples, to keep the consistency of the mixes', a polycarboxylate based superplasticizer have been added to some mixtures. Table 3 shows the characteristics of the superplasticizer.

Table 3: Characteristic of superplasticizer.

Appearance	Brown Liquid
Specific Gravity (20 °C)	1.10 ± 0.03g/ cm ³
pH- value	7.0 ± 1
Alkali Content (%)	≤ 5.0 by mass
Chloride Content (%)	≤ 0.10 by mass
Water Reduction	≥ 112%

Fresh water was used for the preparation of the reference samples according to EN 196-1 :2005 specification. Sea water was supplied from Morecambe Bay in England. Normal sand was supplied from Travis Perkins Group. It is compatible with EN 13139 and its particles size are ≤ 4mm. Sea Sand was collected from Morecambe Bay, and its energy dispersive X-Ray (EDX) and scanning electron microscopy (SEM) samples are shown in Figure 2. It is worth mentioning that the sea sand is not washed before adding to the mortar mixer. Table 4 shows the mix designs of the samples made in this phase of the study. The maximum size of the sea sand particles is 2 mm.

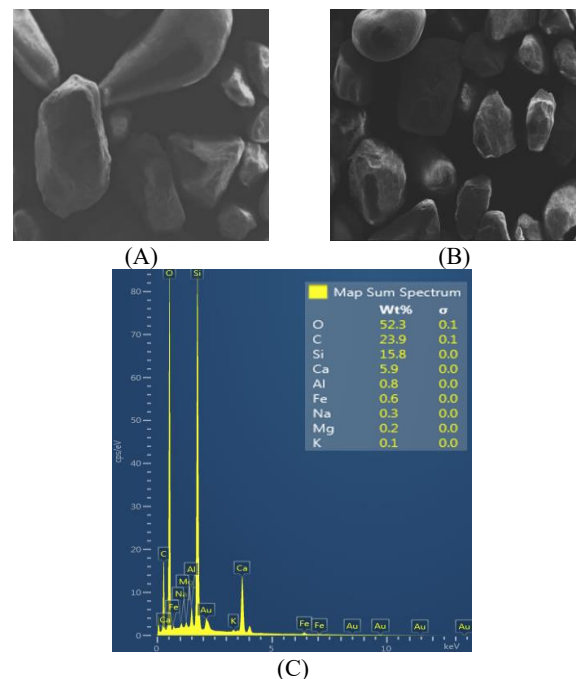


Fig. 2: (A) and (B) are SEM, (C) is EDX for the used sea sand in the mix design.

Table 4: Mix designs of the studied samples incorporating milled and chopped carbon fibre.

Mixtures	REF	Plain ss-sw	1% CF	2% CF	2.5% CF
OPC (g)	720	720	720	720	720
Water (g)	360	-	-	-	-
Sea Water (g)	-	360	360	360	360
Normal Sand (g)	1080	-	-	-	-
Sea Sand (g)	-	1080	1080	1080	1080
W/C	0.5	0.5	0.5	0.5	0.5
Carbon Fibre (g)	-	-	7.2	14.4	18
SP (g)*	-	-	-	3.6	5.4

*Superplasticizer was added to the mixes incorporating only chopped carbon fiber (CCF)

2.2. Mixing Procedure

The reference and the plain ss-sw samples were made following the standard procedure of preparing the cement mortar samples (ASTM C305 – 20). The modified composites were made by following this procedure: First, the dry admixtures (cement, sand, and

carbon fibre) were mixed manually for 3 minutes. Then, 5 minutes mechanically in various speeds to ensure a homogenous dispersion of the solid components. Next, the wet materials of mixtures (superplasticizer, and water) were added together gradually, and the whole mixture was mixed for almost 8 minutes on low and high speeds. Following this procedure resulted in the most homogenous composite in which the fibres were dispersed well. In total, 12 replicates for each mix design were made [12, 14, 16, 17].

Once the fresh mortars were prepared, they were poured into the metallic moulds 40 x 40 x 160 mm and two electrodes with a total extension area of 30*50 mm² were installed in the sample with a distance 120 mm.

The cementitious specimens were left to cure in the moulds at 50 ± 5% RH, 23 ± 2°C for 24 h then removed and placed in a container at the same constant condition until testing.

2.3. Experimental study

To measure the impedance of the samples, the EIS impedance spectroscopy method was employed, using GAMRY Interface instruments shown in Fig.3. The impedance of the samples was tested in various frequencies of an AC signal with the amplitude of 10 mV rms and frequency range starting from 0.1 Hz up to 10 MHz. The impedance was the corresponding real resistance of the sample at the phase angles close to 0 degrees. Hence, each sample has one measured impedance as shown in Fig. 4. This method was adapted from [11, 15].



Fig. 3: EIS potentiostat test set up (Gamry device)

Moreover, once the impedance of the samples is measured, it is used to calculate their resistivity using the following formula:

$$\rho = R \frac{A}{L}$$

In which ρ is the resistivity, R is the measured impedance, L is the distance between the electrodes, and A is the area of the electrodes [15].

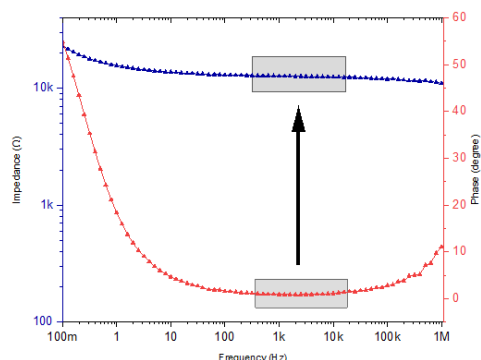


Fig. 4: Impedance and phase of reference sample at day 28 over frequency. The average values of the impedance are calculated relating to the phase values close to zero.

3. The results and discussions

3.1. Electrical conductivity of cementitious mixes

3.1.1. Samples incorporating milled carbon fibre

For each mix design, 12 samples were built and tested. Once the results were taken, each mix design's impedance was calculated by taking the average of all the results.

Fig. 5 shows the evolution of the resistivity of the composite samples over 28 days. The samples were tested in 3 different ages of 7, 14, and 28 days. Milled carbon fibre was introduced in the mixes in 3 different percentages, as mentioned in Table 4.

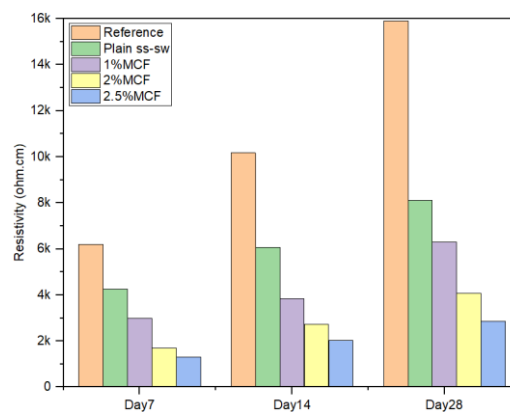


Fig. 5: Resistivity comparison between the reference, plain ss-sw, and MCF samples over time.

As it can be seen, compared to the reference sample, the samples made of sea components have almost 50% less resistivity, which is remarkable and it is mainly because of the sea components being inherently conductive due to considerable sodium crystals ions [18], and can be used to make more conductive concrete without harmful and expensive nano materials. Therefore, the rest of the samples were made incorporating sea components.

Incorporating MCF in the samples, reduces the resistivity remarkably, almost by 60% compared to the plain ss-sw. Incorporating higher percentages of milled carbon fibre has further effects on reducing the resistivity. According to the diagrams, each additional percentage of milled carbon fibre reduces the resistivity by almost 20 to 30%.

In the following section, the conductivity results of the samples with CCF are discussed. Chopped carbon fibers (CCF) were incorporated in 3 different concentrations in the plain ss-sw cement samples made of the sea components.

3.1.2. Samples incorporating chopped carbon fibre

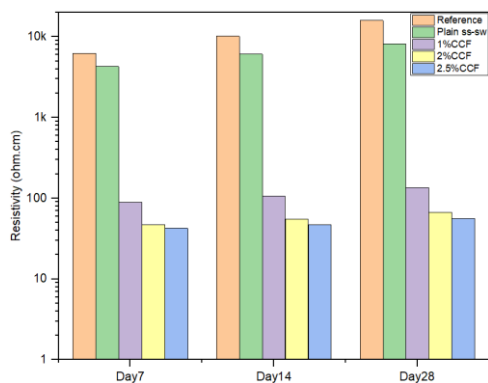


Fig. 6: Resistivity evolution of the reference, plain ss-sw, and CCF samples over time.

Fig. 6 shows the growth of the resistivity of these samples and compares them to the resistivity of the plain ss-sw samples. Regardless of their age and carbon fibre content, all the samples have a resistivity of around 1% of the reference, which is a significant decrease.

The resistivity of the samples increases by time due to the hydration evolution. However, in each age, the resistivity of the samples with 2 and 2.5% of chopped carbon fibre, is almost 50% lower than the 1% samples due to the increased dosage of fibre. An additional reason for these samples' improved resistivity may be the effect of polycarboxylate based admixture (superplasticizer) which has surface active particles, enhancing the electrical properties [19]. It is a necessary admixture to these high CCF content mixes, as without it, the workability would be compromised, and they would not have the same consistency and homogeneity of the rest of the samples. To keep the consistency, superplasticizer was added at the percentages of 0.5% and 0.75% to these mixes (as also detailed in Table 4).

As shown in Fig. 6, regardless of the incorporation percentage, chopped carbon fibre has a significant effect on reducing the resistivity of the samples. Comparing the resistivity results of reference, plain ss-sw, milled and chopped carbon fibre, it is concluded that sea components samples with chopped carbon fibre result in better conductivity. Hence, the experimental study was continued focusing on these samples.

The most intriguing finding is the high effectiveness of the chopped carbon fibres on the electrical properties of mortars. Regardless of the concentration, CCF significantly reduced the resistivity values. At the highest concentration of CCF, resistivity rises from 42.35 Ω cm on day 7 to 53.32 Ω cm on day 28. The presence of high carbon microparticles in CCF (Fig. 1b)

increases their functional electrical surface, resulting in effective conductive paths even at low concentrations. Because of the lower cost and sustainability, the functionality of CCFs at low dosages could provide a strong incentive for the development of high conductive concretes [15, 17, 20].

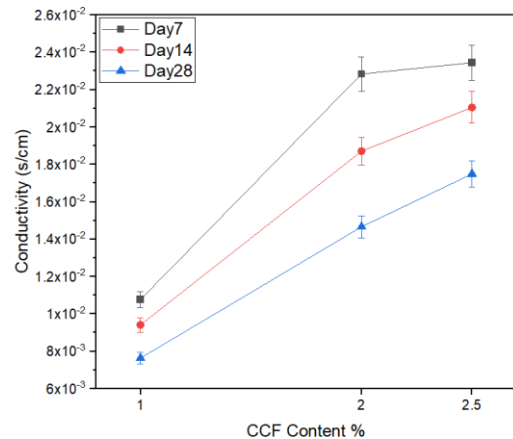


Fig. 7: The electrical conductivity (IS) of mortars vs. the CCF content at day 7, 14, and 28.

Fig. 7 demonstrates the conductivity vs. the chopped carbon fibres concentrations at day 7, 14, and 28 for all the samples, showing the electrical conductivity's enhancement over time by incorporating CCF. It is worth mentioning that an electrical conductivity of cementitious mixes as low as 0.0178 s/cm is a significant improvement [21-23]. In comparison with the MCF only samples, the CCF have dramatic low resistivity.

3.2. Samples' EIS and hydration development results

The Nyquist plot and equivalent circuit simulations of the samples are analysed in this section. The changes in electrical response and the elements of the equivalent circuits over time reflect the cementitious hydration evolution. The frequency range of 0.1 Hz to 1 MHz under an AC signal scans the cementitious composite samples, resulting in the Nyquist plot for each sample. the horizontal axis Z' represents the real part of the impedance and the vertical axis Z'' represents the imaginary part of the impedance. The impedance Z can be calculated by the following equation [24].

$$|Z| = \sqrt{(Z')^2 + (Z'')^2}$$

It is primarily made up of two semi-arcs: (i) the high-frequency arc, which ranges from 100 kHz to 1000 kHz, related to the general characteristics of the nanocomposite, and (ii) the low-frequency arc, which ranges from 0.1 Hz to 100 kHz, related to the characteristics of the stainless-steel electrode's contact with the specimen [25].

The changes in the concentration of ions and charge transfer motion can be precisely recorded by electrochemical impedance spectroscopy. This part used EIS and comparable circuits to discuss how sea water

promotes the hydration of the cementitious composites [13].

The measurement determines the real (resistance) and imaginary (reactance) components of the complex impedance based on the input signal while constantly applying the same voltage to the cement mix over a specified range of alternating current (AC) frequencies [26]. Impedance magnitude, the real part of impedance and the imaginary part of impedance are defined as follows:

$$Z(\omega) = R + jX$$

$$R = |Z(\omega)| \cos \alpha$$

$$X = |Z(\omega)| \sin \alpha$$

$Z(\omega)$ stands for impedance magnitude, ω is operating frequency, j is the imaginary unit, R is the resistance, α is the phase difference between voltage and current (phase shift) and X is the reactance.

3.2.1. Equivalent circuit and hydration development of the reference

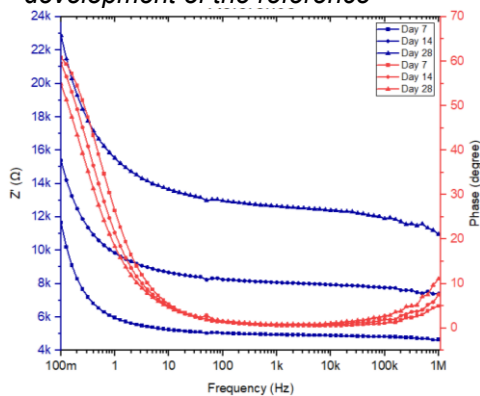


Fig. 8: Reference impedance spectra in Bode plot over frequency with the phase at day 7, 14, and 28.

According to the bode plot and Nyquist, EC should contain three components, including the pore solution and electrodes. For the reference, the proposed equivalent circuit was as follow: $(R_s(C_e(Re\ CPE_e)))$ where R_s represents pore solution resistance, C_e is electrode capacitance, Re electrode resistance, and CPE is constant phase element of electrode.

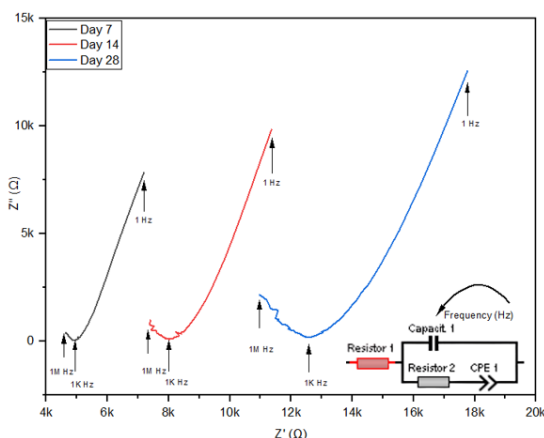


Fig. 9: Reference Nyquist and the equivalent circuit.

3.2.2. Equivalent circuit and hydration of development of plain ss-sw

The proposed equivalent circuit for the results of the plain ss-sw, sea sand and sea water, was as follow: $(R_s(Re\ C_e)(R_{ct}(C_{dl}\ Z_w)))$, double layer capacitance (C_{dl}) and the diffusion behaviour refer to the ion penetration process in the solution Warburg impedance (Z_w) [27, 28]. R_{ct} is the charge transfer impedance. According to Fig. 10, it is clear that sea components have accelerated hydration as the Nyquist plots of the different ages are closer to each other compared to the reference.

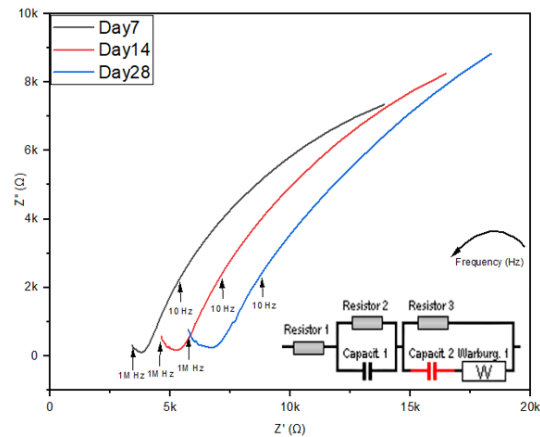


Fig. 10: Plain ss-sw Nyquist and the equivalent circuit.

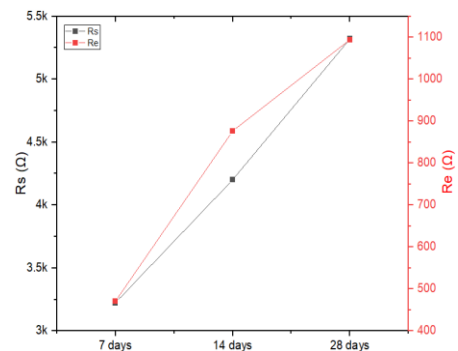


Fig. 11: Plain ss-sw equivalent circuit R_s (pore solution), R_e (Electrode).

In Fig. 11 the evolution of R_e and R_s is shown by time. Both parameters show a steady growth as the sample cures.

3.2.3. Equivalent circuit and hydration of development of CCF

A proposed equivalent circuit was used for all concentrations of CCF. Constant phase element (CPE) has been added to the EC, The CPE behaviour can be viewed as the frequency dispersion of capacitance due to dielectric relaxation, where the electric current density follows the change of an electric field with a delay [29]. According to Figure 12, it is obvious that CCF converted the cement-based composite from an insulator to highly conductive material due to the smaller semicircles throughout all the frequencies which indicates a great reduction in the compound resistance. The proposed EC is $(R_s(CPE_e\ Re)(C_{dl}\ R_{ct}))$.

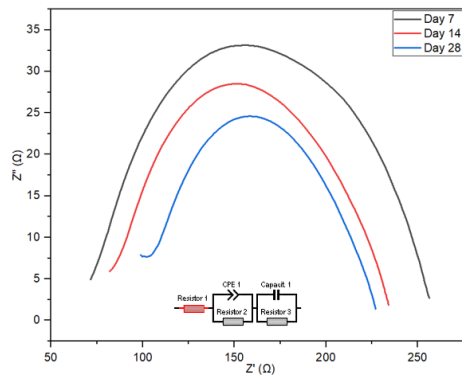


Fig. 12: 1% CCF Nyquist and the equivalent circuit.

The following figures show the resistance components of the mentioned equivalent circuit of the CCF vs concentration and age.

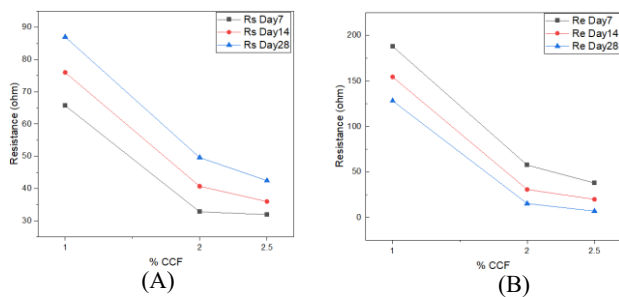


Fig. 13: CCF equivalent circuit A) R_s (pore solution), B) R_e (Electrode).

3.3. Self-sensing properties of the samples

A self-sensing procedure was developed at the end of a curing period (1 year) to examine the cement-based mortars containing various percentages of chopped carbon fibre. Compression loads were used as inputs and electrical resistivity measurements were used as outputs to evaluate the self-sensing properties. The axial load was applied by using INSTRON testing machine with a load bearing capacity of 100 kN, operating under force control. The applied loads were controlled, and a GAMRY Interface instrument was used to measure the electrical impedance (EIS) under each mechanical load.

In order to test the samples, the load was applied to the marginal base of the samples along with its longitudinal axis with an application area of $40 \times 40 \text{ mm}^2$ as shown in Fig. 14. In each test, there were six loading cycles with force control at a speed of 100 N/s. Each sample was first placed in the testing set up and its impedance was measured while completely unloaded. Then, the loading process would start, until the assigned target load, which when achieved, the loading would be paused, and another impedance measurement was conducted. The on-hold period (almost 5 minutes) would continue until a full impedance measurement and once done, the loading process would resume until the next target load. To avoid any interference in the measurement of the electrical tests, a thin rubber sheet was positioned between the specimen and the testing machine plates. Tests were conducted on samples for each mix design

(1%, 2%, 2.5% CCF) with the average results provided. The method was adapted from [11].

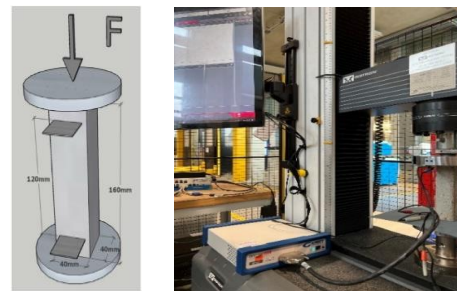


Fig. 14: Self-sensing test set up.

As shown in Fig. 14, self-sensing test was conducted by varying the loads applied on the specimen while measuring the EIS with the frequency ranging between 1 kHz to 100kHz. This frequency is within the resistive reactance range of the tested specimens, so it is appropriate for such measurements [11, 30].

Moreover, it was observed that introducing chopped carbon fibres (CCF) to the mixes, changes this pattern significantly and the samples show remarkable sensitivity to the applied mechanical loads. The results of these samples are shown in Fig. 15.

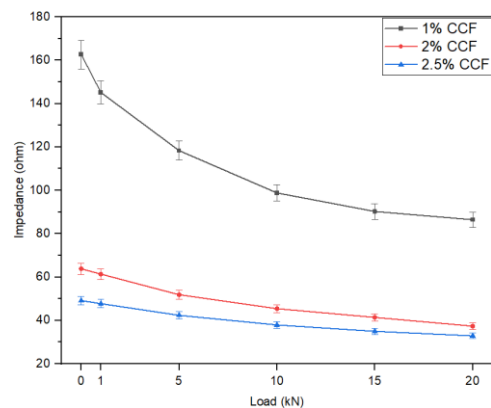


Fig. 15: Impedance over load for CCF mixes.

Fig. 15 demonstrate the sensitivity of the cement reinforced with chopped carbon fibre. Even though the concentrations are low, such as 1% CCF, it shows a great potential for sensitivity and for example to detect a damage in structural health. As shown, while the loads were applying and increasing, the impedance decreases as a response to each load. In 1% CCF samples, the impedance for 0 kN condition and applying 1 kN condition are 165 ohms and 146 ohms respectively whereas when applying 20 kN on the marginal base the impedance becomes 90 ohms which means around half of the unloaded impedance. The impedance response of all samples incorporating CCF, regardless of their percentage, meaningfully changes under different mechanical loads. In both cases, by increasing the magnitude of the load, the impedance response decreases. The impedance reduction of 35% to 45% is noticed for each dosage. Therefore, it is concluded that incorporating CCF in cementitious mixes increases their self-sensing properties.

4. Conclusion

The aim of this paper is to investigate the possibility of building a smart and sustainable cementitious composite. The effect of using sea sand and seawater (plain ss-sw) instead of fresh water and normal sand (reference) has improved the mixes in terms of their electrical properties, hydration, along with being a more sustainable option. The effect of chopped and milled carbon fibres on the conductivity and self-sensing properties of the samples after 1 year of curing is studied. The main outcomes of this study are summarized as the following:

- Using sea sand and sea water (plain ss-sw) have improved the electrical conductivity by almost 50% compared to the mixes with fresh water and normal sand (reference).
- Adding milled carbon fibre results in reduction of the resistivity by 35-60% depending on the fibres content.
- Incorporating chopped carbon fibre enhances the electrical properties significantly, regardless of the concentration, as it shows a stabilization at 53 Ω cm after 1 year of curing. The electrical conductivity of the reference and plain ss-sw mix after one year are 256k Ω cm and 170k Ω cm, respectively.
- Samples incorporating chopped carbon fibres showed a strong self-sensing feature tested on the samples after 1 year of curing. In the case of 2.5% CCF sample, by increasing the mechanical loads from 0 to 20 kN the impedance goes from 50 to 32 ohm.

Finally, it is shown that the cementitious composites incorporating carbon fibres have a high potential of being employed in the smart city infrastructures specifically for health monitoring and data transmissions applications.

The authors gratefully acknowledge the financial support provided by Jouf University to make this research possible at Lancaster University.

References

- [1] United Nations Environment Programme, "Sand and sustainability UNEP 2019," *UNEP. Sand and sustainability*, 2019.
- [2] "Readily implementable techniques can cut annual CO₂ emissions from the production of concrete by over 20%," 2016, doi: 10.1088/1748-9326/11/7/074029.
- [3] T. Dhondy, A. Remennikov, and M. N. Shiekh, "Benefits of using sea sand and seawater in concrete: a comprehensive review," *Australian Journal of Structural Engineering*, vol. 20, no. 4, pp. 280–289, 2019. doi: 10.1080/13287982.2019.1659213.
- [4] T. Jose, M. P. Benny, and U. G. Scholar, "Feasibility of Sea-Sand Sea-Water Concrete," vol. 8, no. 08, pp. 18–25, 2019.
- [5] J. Xiao, C. Qiang, A. Nanni, and K. Zhang, "Use of sea-sand and seawater in concrete construction: Current status and future opportunities," *Constr Build Mater*, vol. 155, pp. 1101–1111, 2017, doi: 10.1016/j.conbuildmat.2017.08.130.
- [6] U. Ebead, D. Lau, F. Lollini, A. Nanni, P. Suraneni, and T. Yu, "A review of recent advances in the science and technology of seawater-mixed concrete," *Cem Concr Res*, vol. 152, Feb. 2022, doi: 10.1016/j.cemconres.2021.106666.
- [7] P. Li, W. Li, Z. Sun, L. Shen, and D. Sheng, "Development of sustainable concrete incorporating seawater: A critical review on cement hydration, microstructure and mechanical strength," *Cem Concr Compos*, vol. 121, no. May, p. 104100, 2021, doi: 10.1016/j.cemconcomp.2021.104100.
- [8] A. Dasar, D. Patah, H. Hamada, Y. Sagawa, and D. Yamamoto, "Applicability of seawater as a mixing and curing agent in 4-year-old concrete," *Constr Build Mater*, vol. 259, p. 119692, 2020, doi: 10.1016/j.conbuildmat.2020.119692.
- [9] T. Dhondy, A. Remennikov, and M. N. Shiekh, "Benefits of using sea sand and seawater in concrete: a comprehensive review," *Australian Journal of Structural Engineering*, vol. 20, no. 4, pp. 280–289, 2019. doi: 10.1080/13287982.2019.1659213.
- [10] H. Allam, F. Duplan, S. Amziane, and Y. Burtshell, "Assessment of manufacturing process efficiency in the dispersion of carbon fibers in smart concrete by measuring AC impedance," *Cem Concr Compos*, vol. 127, Mar. 2022, doi: 10.1016/j.cemconcomp.2021.104394.
- [11] J. Donnini, T. Bellezze, and V. Corinaldesi, "Mechanical, electrical and self-sensing properties of cementitious mortars containing short carbon fibers," *Journal of Building Engineering*, vol. 20, pp. 8–14, Nov. 2018, doi: 10.1016/j.jobe.2018.06.011.
- [12] S. Erdem, S. Hanbay, and M. A. Blankson, "Self-sensing damage assessment and image-based surface crack quantification of carbon nanofibre reinforced concrete," *Constr Build Mater*, vol. 134, pp. 520–529, 2017, doi: 10.1016/j.conbuildmat.2016.12.197.
- [13] D. D. L. Chung, "Self-monitoring structural materials," *Materials Science and Engineering R: Reports*, vol. 22, no. 2, pp. 57–78, 1998, doi: 10.1016/S0927-796X(97)00021-1.
- [14] N. Banthia, S. Djerdane, and M. Pigeon, "ELECTRICAL RESISTIVITY OF CARBON AND STEEL MICRO-FIBER REINFORCED CEMENTS," *Cem Concr Res*, vol. 5, no. 1, pp. 1–8, 1992, [Online]. Available: <https://ejournal.poltektegal.ac.id/index.php/siklus/article/view/298%0Ahttp://repositorio.unan.edu.ni/2986/1/5624.pdf%0Ahttp://dx.doi.org/10.1016/j.jana.2015.10.005%0Ahttp://www.biomedcentral.com/1471->

- 2458/12/58%0Ahttp://ovidsp.ovid.com/ovidweb.cgi?T=JS&P
- [15] A. Belli, A. Mobili, T. Bellezze, and F. Tittarelli, "Commercial and recycled carbon/steel fibers for fiber-reinforced cement mortars with high electrical conductivity," *Cem Concr Compos*, vol. 109, no. September 2019, p. 103569, 2020, doi: 10.1016/j.cemconcomp.2020.103569.
- [16] H. Nguyen, V. Carvelli, T. Fujii, and K. Okubo, "Cement mortar reinforced with reclaimed carbon fibres, CFRP waste or prepreg carbon waste," *Constr Build Mater*, vol. 126, pp. 321–331, 2016, doi: 10.1016/j.conbuildmat.2016.09.044.
- [17] A. Al-Dahawi, F. Emami, G. Yildirim, and S. Mustafa, "Effect of mixing methods on the electrical properties of cementitious composites incorporating different carbon-based materials," vol. 104, pp. 160–168, 2016, doi: 10.1016/j.conbuildmat.2015.12.072.
- [18] L. Montanari, P. Suraneni, and M. T. Chang, "Hydration , Pore Solution , and Porosity of Cementitious Pastes Made with Seawater," no. May, 2019, doi: 10.1061/(ASCE)MT.1943-5533.0002818.
- [19] F. Yousuf, X. Wei, and J. Tao, "Evaluation of the influence of a superplasticizer on the hydration of varying composition cements by the electrical resistivity measurement method," *Constr Build Mater*, vol. 144, pp. 25–34, Jul. 2017, doi: 10.1016/j.conbuildmat.2017.03.138.
- [20] F. Emami, G. Yildirim, and S. Mustafa, "Effect of mixing methods on the electrical properties of cementitious composites incorporating different carbon-based materials," vol. 104, pp. 160–168, 2016, doi: 10.1016/j.conbuildmat.2015.12.072.
- [21] H. Yu, Y. Lei, C. Pei, L. Wei, J. H. Zhu, and F. Xing, "Enhancing the mechanical and functional performance of carbon fiber reinforced cement mortar by the inclusion of a cost-effective graphene nanofluid additive," *Cem Concr Compos*, vol. 134, Nov. 2022, doi: 10.1016/j.cemconcomp.2022.104777.
- [22] B. Chen, K. Wu, and W. Yao, "Conductivity of carbon fiber reinforced cement-based composites," *Cem Concr Compos*, vol. 26, no. 4, pp. 291–297, May 2004, doi: 10.1016/S0958-9465(02)00138-5.
- [23] W. Pichór, M. Fraç, and M. Radecka, "Determination of percolation threshold in cement composites with expanded graphite by impedance spectroscopy," *Cem Concr Compos*, vol. 125, no. February 2021, 2022, doi: 10.1016/j.cemconcomp.2021.104328.
- [24] F. Rajabipour, J. Weiss, J. D. Shane, T. O. Mason, and S. P. Shah, "Procedure to Interpret Electrical Conductivity Measurements in Cover Concrete during Rewetting", doi: 10.1061/ASCE0899-1561200517:5586.
- [25] McCarter and Brousseau, "THE A.C. RESPONSE OF HARDENED CEMENT PASTE," *Cem Concr Res*, vol. 20, 1990.
- [26] D. D. L. Chung, "Electrically conductive cement-based materials," no. 4, pp. 167–176, 2004.
- [27] K. M. Emran and H. AL-Refai, "Electrochemical and surface investigation of Ni-Cr glassy alloys in nitric acid solution," *Int J Electrochem Sci*, vol. 12, no. 7, pp. 6404–6416, Jul. 2017, doi: 10.20964/2017.07.43.
- [28] N. Naderi, M. R. Hashim, K. M. A. Saron, and J. Rouhi, "Enhanced optical performance of electrochemically etched porous silicon carbide," *Semicond Sci Technol*, vol. 28, no. 2, Feb. 2013, doi: 10.1088/0268-1242/28/2/025011.
- [29] S. Sen and P. K. Dutta, "Realization of a Constant Phase Element and Its Performance Study in a Differentiator Circuit," *IEEE Transactions on Circuits and Systems II: Express Briefs*, vol. 53, no. 9, pp. 802–806, 2006, doi: 10.1109/TCSII.2006.879102.
- [30] B. Han, S. Ding, and X. Yu, "Intrinsic self-sensing concrete and structures: A review," *Measurement*, vol. 59, pp. 110–128, Jan. 2015, doi: 10.1016/J.MEASUREMENT.2014.09.048.